Published in final edited form as:
Radiat Environ Biophys. 2019 May ; 58(2): 215–226. doi:10.1007/s00411-019-00785-2.

Influence of the external and internal radioactive contamination of the body and the clothes on the results of the thyroidal ^{131}I measurements conducted in Belarus after the Chernobyl accident. Part 2: Monte Carlo simulation of response of detectors near the thyroid

Semion Kutsen,
Institute for Nuclear Problems, Belarusian State University, Minsk, Belarus

Arkady Khrutchinsky,
Institute for Nuclear Problems, Belarusian State University, Minsk, Belarus

Victor Minenko,
Institute for Nuclear Problems, Belarusian State University, Minsk, Belarus

Paul Voillequé,
MJP Risk Assessment, Inc., Denver, CO, USA

André Bouville, and
U.S. National Cancer Institute (retired), Bethesda, MD, USA

Vladimir Drozdovitch
Division of Cancer Epidemiology and Genetics, National Cancer Institute, NIH, DHHS, 9609, Medical Center Drive, Room 7E548 MSC 9778, Bethesda, MD 20892-9778, USA.

Abstract

This paper describes the calculation of the response of the most common types of radiation detectors that were used within the first few weeks after the Chernobyl accident to determine the activity of ^{131}I in the thyroids of Belarusian subjects of an epidemiologic study of thyroid cancer. The radiation detectors, which were placed against the necks of the subjects, measured the exposure rates due to the emission of gamma rays resulting from the radioactive decay of ^{131}I in their thyroids. Because of the external and internal radioactive contamination of the monitored subjects, gamma radiation from many radionuclides in various locations contributed to the exposure rates recorded by the detectors. In order to estimate accurately the contribution from gamma rays emitted from various internal and external parts of the body, the calibration factors of the radiation detectors, expressed in kBq per μR h^{-1}, were calculated, by means of Monte Carlo simulation, for external irradiation from unit activities of 17 radionuclides located on 19 parts of the body, as well as for internal irradiation from the same 17 radionuclides in the lungs, from caesium radionuclides distributed uniformly in the whole body, and from ^{131}I in the thyroid. The calculations were performed for six body sizes, representative of the age range of the subjects. In a

Phone: +1-240-276-7399, Fax: +1-240-276-7840; drozdovv@mail.nih.gov.

companion paper, the levels of external and internal contamination of the body were estimated for a variety of exposure conditions. The results presented in the two papers were combined to calculate the ^{131}I activities in the thyroids of all 11,732 Belarusian study subjects of an epidemiologic study of thyroid cancer and, in turn, their thyroid doses.

Keywords

Chernobyl; thyroid; 131I measurement; external contamination; internal contamination

Introduction

The accident at the Chernobyl nuclear power plant in April 1986 resulted in widespread radioactive contamination of the territories of Belarus, the Russian Federation, and Ukraine. Most of the radiation exposure to the affected population resulted from the intake of radioisotopes of iodine, especially ^{131}I (UNSCEAR 2011). The U.S. National Cancer Institute has initiated in Belarus and Ukraine a long-term cohort study of thyroid cancer among 25,000 persons exposed in childhood to radioactive fallout from the Chernobyl accident (Stezhko et al. 2004). The reconstruction of the individual doses for the cohort members is based on so-called “direct thyroid measurements”, which consisted of measurements of exposure rates against the necks of the study subjects and were performed during the few first weeks after the accident in Belarus (Gavrilin et al. 1999) and Ukraine (Likhtarev et al. 1993). The ^{131}I activities in the thyroid glands of the study subjects were then derived from the measured exposure rates.

In Belarus, the direct thyroid measurements were predominantly performed using two types of radiation devices that were not originally intended to measure activity levels in humans: (1) the DP-5 device, with a Geiger-Mueller (GM) counter, which was designed for use by military and civil defense organizations; about 55% of the cohort members were measured with this device, and (2) the SRP-68–01 device, which is a NaI(Tl) scintillation survey-meter that was commonly used in the former Soviet Union for geological exploration; about 40% of the measurements of the cohort members were made with a SRP-68–01 device.

Most of the direct thyroid measurements were performed in contaminated Belarusian villages under such conditions that the radiation signal included, in addition to the gamma rays emitted during the decay of the ^{131}I present in the thyroid, two additional components that had to be taken into consideration. One of these components is the room background, which includes the natural background radiation and the radioactive contamination due to the Chernobyl accident in the room where the subject was measured. According to the measurement protocol, the room background should have been measured systematically. Unfortunately, often the room background was either not recorded or not measured. The methods used to estimate the room background for each group of subjects measured at a particular location and date are described in a separate publication (Drozdovitch et al. 2013). The other component of the radiation signal arose from the fact that the subject may have worn contaminated clothes, may not have washed herself or himself properly before the measurement, and may have inhaled or ingested radioactive material released during the

Chernobyl accident. It is therefore important to estimate the background due to external and internal contamination of the body and clothes, which, unfortunately, was rarely monitored. Measures that could have been taken include equipping the SRP-68–01 devices with lead collimators, as was done in Ukraine (Likhtarev et al. 1995), or measuring the background exposure rate near the thigh of the subject to account for the contribution of Cs isotopes in the body to the detector response (Zvonova et al. 1998).

The purpose of the present paper is to evaluate the response of the thyroid detectors used at that time to unit activities of radionuclides either deposited on clothes and body surfaces or incorporated in the body. In a companion paper (Drozdovitch et al. 2019, this issue), models describing the external and internal radioactive contamination of the human body resulting from the Chernobyl accident are presented and absolute activities are calculated. The combination of the results obtained in the two papers made it possible to estimate more accurately the ^{131}I contents in the thyroids of the 11,732 members of the Belarusian cohort and resulted in the improvement of their individual thyroid dose estimates (Drozdovitch et al. 2013, 2015).

Materials and methods

The materials and methods used to estimate the calibration factors of the two types of radiation detectors (DP-5 and SRP-68–01) for the two types of contamination are described in this section.

Calibration factor for the surface contamination of the body and clothes

For the purpose of the estimation of thyroid doses for the cohort members of the epidemiologic study, the calibration factor for surface contamination of the body and clothes was estimated for 17 of the most commonly encountered gamma-ray emitting radionuclides that were released into the atmosphere during the Chernobyl accident, ^{95}Zr, ^{95}Nb, ^{99}Mo, ^{103}Ru, ^{106}Ru, ^{132}Te, ^{131}I, ^{132}I, ^{133}I, ^{134}Cs, ^{136}Cs, ^{137}Cs, ^{140}Ba, ^{140}La, ^{141}Ce, ^{144}Ce, and ^{239}Np (radionuclides are listed according to increasing mass number, not according to their importance) for six age groups from newborn to adult that represent a family of Oak Ridge National Laboratory (ORNL) phantoms (Cristy 1980; Cristy and Eckerman 1987). Figure 1 shows the division of the ORNL phantom body-surface into the 19 regions according to a special modification of the ORNL phantom (Ulanovsky et al. 2004). The areas of the body surface regions for the six age-dependent phantoms are given in Table 1. The activities of the gamma-emitting radionuclides were assumed to be distributed uniformly over each of the body surface regions. The legs and shoes were not considered in this study as the contribution of their surface contamination to the response of the detector, which was located against the thyroid, was found to be less than 0.01% of the total readout.

The relationship between the calibration factor and the exposure rate due to external contamination of clothes and human body surface was expressed as follows (Eq. 1): where

$$ER_{i,j,k}^{ext} = \frac{\sigma_{i,j,k} \times s_{j,k}}{CF_{i,j,k}^{ext}}, \quad (1)$$

where $ER_{i,j,k}^{ext}$ is the exposure rate measured near the thyroid that is due to radionuclide i on body surface region j of a subject in age group k (μR h^{-1}); $\sigma_{i,j,k}$ is the surface density of radionuclide i on body surface region j (kBq cm^{-2}); $s_{j,k}$ is the size of body surface region j (cm^2) (see Fig. 1 and Table 1); $CF_{i,j,k}^{ext}$ is the calibration factor of the thyroid detector for radionuclide distributed on body surface region j (kBq per μR h^{-1}). The indices i, j, k are used here and elsewhere in the paper to indicate, respectively, the radionuclide, the body surface region, and the age group being considered.

The calibration factor of the detector is defined as the activity of radionuclide i per unit exposure rate measured by the detector placed near the thyroid (see Fig. 1); it is calculated as:

$$CF_{i,j,k}^{ext} = 10^{-3} \cdot \frac{SC}{\eta_{i,j,k}}, \quad (2)$$

where SC is the device-specific scale coefficient (counts s^{-1} per μR h^{-1}); the value of SC, which is determined only by the electronic scheme of the device, does not depend on either the gamma-ray energy or the measurement geometry; $\eta_{i,j,k}$ is the total efficiency of the detector for detection of gamma rays, i.e. the number of photons registered by the detector located near the thyroid per unit activity of radionuclide i on body surface region j (counts s^{-1} per Bq).

Usually, the decay scheme of radionuclide i includes several gamma rays of different energies and yields, so that the efficiency of the detector for that radionuclide is calculated as:

$$\eta_{i,j,k} = \sum_n p_i(E_n) \cdot \eta_{j,k}(E_n), \quad (3)$$

where $p_i(E_n)$ (unitless) is the yield of photon emission per decay with energy E_n for radionuclide i, based on the 2003 update of information of ICRP Publication 38 (ICRP 1983); $\eta_{j,k}(E_n)$ is the energy-specific efficiency for detection of photon of energy E_n emitted from body surface region j; the values of $\eta_{j,k}(E_n)$ were determined for selected energies ranging from 0.025 to 3 MeV, the two types of radiation detectors, the six phantoms representing the age range of the study subjects, and the 19 regions of the human body.

It follows from Eqs. (1) to (3) that most of the parameter values were already available and that only the values SC and of $\eta_{j,k}(E_n)$ needed to be obtained in order to determine the values of the calibration factor $CF_{i,j,k}^{ext}$ for the two radiation detectors and a range of conditions:

- The values of the device-specific scale coefficient, *SC*, expressed in counts s^{-1} per μR h^{-1}, were determined experimentally. For the DP-5 devices, sources of ^{60}Co (main photon energy of 1.173 and 1.332 MeV (ICRP 2008)), ^{137}Cs (0.6617 MeV), and ^{241}Am (0.0263 and 0.0595 MeV) were placed at various distances from the detector. The exposure rates were read on one of the scales, which ranged up to 10,000 μR h^{-1}, while the count rates were recorded using a pulse counter in a parallel channel. Results of measurements done by the DP-5 of the exposure rates and the count rates obtained using a plastic phantom of the neck and thyroid with ^{133}Ba (0.081, 0.276, 0.3029, 0.356 and 0.3838 MeV) source were also used to determine the scale coefficient. The values of *SC* for the SRP-68–01, which were determined using a similar protocol, were previously published (Khrutchinsky et al. 2012).

- The values of the energy-specific efficiency $\eta_{j,k}(E_n)$, expressed in counts per photon, were calculated using a family of ORNL human phantoms (representing the newborn; children aged 1 y, 5 y, 10 y, 15 y; and adults) and a Monte Carlo simulation of radiation transport from the considered body surface to the radiation detector located against the thyroid. The ORNL phantoms were modified to make their neck areas more realistic anatomically (Ulanovsky and Eckerman 1998) and to use an improved mathematical model of the thyroid (Ulanovsky et al. 1997). In the calculations, the internal structure of the phantoms (except for lungs, trachea, and thyroid) was not considered and, therefore, it was assumed that the phantoms have a uniform density of 1.04 kg m^{-3}. The density of the lungs was taken to be 0.296 kg m^{-3} according to (Cristy and Eckerman 1987). Table 2 provides the age-dependent volumes of phantoms' whole body (including legs), lung and thyroid gland that were used in the calculations (Cristy and Eckerman 1987; Ulanovsky et al. 1997; Ulanovsky and Eckerman 1998). The values of the energy-specific efficiency were calculated for the so-called "standard" position of the detector used in the direct thyroid measurements, e.g. when the detector is located against the thyroid, at the lower point of the neck.

- The DP-5 device utilizes a Geiger-Mueller (GM) counter which detects the charged particles that occur inside the working volume of the counter. The efficiency of detecting charged particles by the GM counter is close to 100 %. For the direct thyroid measurements, only the gamma radiation was measured as the GM counter was located inside the metal probe of the DP-5 device. The GM counter is able to detect gamma quanta which generate secondary charged particles on its walls. Each charged particle that reached the working volume of a GM counter is caused by the interaction of a gamma quantum with a wall of the GM counter. The operation of the GM counter as a gas-filled detector working in the self-discharge mode cannot be simulated directly using Monte Carlo code. If one assumes that any charged particle that reached the working volume of the

GM detector was counted, then the signal from the counter is proportional to the total number of electrons inside the working volume. This number was calculated by Monte Carlo simulations which were carried out by means of the MCNP-4B code (Briesmeister 1994).

- It should be noted that the detection efficiency of gamma radiation by a GM counter is around three orders of magnitude less than that by a scintillation detector. To restrict the duration of the simulations of the DP-5 response to the surface radiation source to a manageable level, a statistical uncertainty of Monte Carlo simulation of 5–7 % was accepted for the DP-5 while 1–2% was the goal for the SRP-68–01 detector. The mathematical modeling of the SRP-68–01 survey-meter is described in detail elsewhere (Khrutchinsky et al. 2012).
- A detailed mathematical description of the approach developed and other means to improve the calculation efficiency are given in Appendix.

Calibration factor for internal contamination of the body

To estimate the thyroid doses for the subjects of the epidemiologic study, the calibration factors for internal contamination of the body were calculated (a) for ^{131}I in the thyroid, (b) for lung burdens of each of the 17 radionuclides identified previously, and (c) for caesium radionuclides (^{134}Cs, ^{136}Cs and ^{137}Cs) in the whole body. The calculations were made for the two types of radiation detectors and for six age groups from newborn to adult.

By analogy to Eq. (1) for external irradiation, the exposure rate due to radionuclide activities in the thyroid or the lungs is given by the following equation (Eq. 4):

$$ER_{i,m,k}^{int} = \frac{A_{i,m,k}}{CF_{i,m,k}^{int}}, \quad (4)$$

where $ER_{i,m,k}^{int}$ is the exposure rate (μR h^{-1}) due to the activity $A_{i,m,k}$ (kBq) of radionuclide i assumed to be uniformly distributed in the source organ m of a subject in age group k; and $CF_{i,m,k}^{int}$ is the calibration factor of the thyroid detector for radionuclide i incorporated in the source organ m of a subject in age group k (kBq per μR h^{-1}).

The calibration factor of the detector for internal contamination of the thyroid or lungs is defined as the activity of radionuclide i in the source organ under consideration per unit exposure rate measured by the detector near the thyroid. The calibration factor is calculated as:

$$CF_{i,m,k}^{int} = 10^{-3} \cdot \frac{SC}{\eta_{i,m,k}}, \quad (5)$$

where SC is the device-specific scale coefficient (counts s^{-1} per μR h^{-1}); $\eta_{i,j,k}$ is the total efficiency of the detector for gamma rays emitted by radionuclide i located in the source organ *m* (thyroid or lungs) of a person of age *k*, i.e. the number of photons registered by the detector located near the thyroid normalized to the total number of disintegrations in the organ (counts s^{-1} per Bq).

In the same way as for external irradiation, the total efficiency of the detector to a radiation source with a complex energy spectrum was calculated as:

$$\eta_{i,m,k} = \sum_n p_i(E_n) \cdot \eta_{m,k}(E_n), \quad (6)$$

In the case of the caesium radionuclides distributed within the whole body, a different approach was used to calculate the calibration factors. First, legs were added to the whole-body phantom. Second, because the parts of the body distant from the thyroid may not contribute substantially to the detector response because of complete absorption of the emitted gamma rays by intervening tissues, the readout of the device was modeled by first considering the parts of the body nearest the detector and then gradually increasing the volume considered until a maximal value (V^*) was reached when either further additions no longer increased the readout of the device or the entire volume of the body was scanned.

The quantity *CF* is volume-dependent, *CF(V)*, in the same way as, for example, the total activity of a radioactive liquid with a constant volumetric activity depends on the volume of the sample taken. Therefore, a volumetric calibration factor, $CF^{int\,*}_{Cs,\,body,\,k}$ (kBq cm^{-3} per μR h^{-1}) was used in this study. It is defined as:

$$CF^{int\,*}_{Cs,\,body,\,k} = 10^{-3} \cdot \frac{SC}{\eta^{*}_{Cs,\,body,\,k}}, \quad (7)$$

where $\eta^{*}_{Cs,\,body,\,k} = \eta^{*}_{Cs,\,body,\,k}(V^*) \cdot V^{*}_{k}$ is the integral device response to the source of radiation uniformly distributed within volume, V^{*}_{k}, of the source in the body of a subject of age group *k* (count s^{-1} cm^3 per Bq).

The volumetric calibration factor would be more representative since it does not depend on volume. The relation between the calibration factor, $CF^{int}_{Cs,\,body,\,k}$, and the volumetric calibration factor for whole body, $CF^{int\,*}_{Cs,\,body,\,k}$, is given by the following equation (Eq. 8):

$$CF^{int}_{Cs,\,body,\,k} = CF^{int\,*}_{Cs,\,body,\,k} \cdot V_k, \quad (8)$$

where V_k is the volume of the whole body of a subject of age group *k* (cm^3).

It follows from Eqs. (4) to (7) that most of the parameter values were already available and that only the values $\eta_{i,m,k}$ for internal irradiation from the thyroid and lungs, and of $\eta^{*}_{Cs,\,body,\,k}$ for internal irradiation from caesium radionuclides within the whole body need to be obtained in order to determine the values of the calibration factor, $CF_{i,m,k}^{int}$, for the two radiation detectors and a range of conditions:

- The values of the energy-specific efficiency, $\eta_{m,k}(E_n)$, expressed in counts per photon, were calculated using Monte-Carlo simulation of radiation transport from the considered organ (thyroid or lungs) to the radiation detector located against the thyroid.
- The values of $\eta^{*}_{Cs,\,body,\,k}$ and V_k^{*} needed for the estimation of the calibration factors for the caesium radionuclides in the whole body were calculated using the truncation procedure to eliminate the distant photons that do not reach the detector. The volumetric calibration coefficient based on the integral response does not depend on the size of the volume source and is determined by the volumetric activity. The main contribution to detector response is caused by the trunk regions closest to the detector. Therefore, it is possible to truncate the trunk at any distance from the detector position and consider the distance “detector – truncating plane” as an “extension” of the region of interest. Using the integral device response, which increases with the extension of the region of interest until reaching a plateau, it was possible to find the value of the maximal volume V_k^{*} for which the integral device response does not increase any more.

Results and discussions

Device-specific scale coefficient

As previously mentioned, the values of the device-specific scale coefficient, *SC*, were determined experimentally, in cooperation with the Scientific and Production Enterprise (SPE) “Atomtex” (Minsk, Belarus), using the dose testing installation UIEZ-001 with a verification certificate issued by the Mendeleyev Institute of Metrology (Saint Petersburg, Russia). According to the DP-5 certificate, the tests should be performed with a ^{226}Ra gamma-radiation source. However, the experience gained after 1986 showed that it was sufficient to use a ^{60}Co gamma radiation source and to place the detector at various distances from the source in a plane-parallel field of radiation that correspond to known values of the exposure rate. In addition, sources of ^{137}Cs and ^{241}Am were used to confirm the value of the scale coefficient obtained with ^{60}Co. Results of measurements done by the DP-5 of the exposure rates and the count rates obtained using a plastic phantom of the neck and thyroid with a ^{133}Ba source were also used to determine the scale coefficient. The values of the device-specific scale coefficient obtained experimentally using the different radiation sources are shown in Table 3. The mean and standard deviation of the scale coefficient were found to be 0.020 and 0.002 (counts s^{-1} per μR h^{-1}), respectively, for the instruments tested.

For the survey-meter SRP-68–01, the value of the scale coefficient determined experimentally in a separate study (Khrutchinsky et al. 2012) using a ^{22}Na source was 3.68 (counts s^{-1} per μR h^{-1}) for the detector that was tested.

Calibration factor

External irradiation—The calibration factors for the DP-5 and the SRP-68–01 devices were calculated for the considered radionuclides distributed over the 19 body surface regions of human phantoms representative of six age groups. Front of neck (surface #3), being the closest location to the thyroid detector, was found to be the main contributor to the response of both detectors. Figures 2 and 3 show the energy-specific efficiency, $\eta_{m,k}$, of the DP-5 and the SRP-68–01 devices, respectively, for photons with energy E_n distributed on the front of the neck (surface #3) of individuals of different ages. As expected, the energy-specific efficiencies of both devices decrease with the age of the person. Tables 4 and 5 present the calibration factors calculated, as examples, for a five years old child for the DP-5 and the SRP-68–01 devices, respectively. Calibration factors for ^{99}Mo,^{106}Ru, and ^{144}Ce include the contributions from gamma-rays of short-lived progenies: ^{99m}Tc, ^{106}Rh, and ^{144}Pr, respectively.

Uncertainties in the values of the calibration factors presented in Tables 4 and 5 are defined by the variability of the scale coefficients for the DP-5 and the SRP-68–01 devices and statistical uncertainties of Monte Carlo calculations of total efficiency of the detectors for gamma rays. The simplifying assumption was made that all children in the same age group have the same morphology as the ORNL human phantom representing that age group. Relative uncertainties in calibration factors are in the ranges from 0.10 to 0.12 and 0.06 to 0.08 for the DP-5 and SRP-68–01 devices, respectively.

Internal irradiation—Table 6 gives the age-dependent calibration factors calculated in the present study for the DP-5 and the SRP-68–01 devices in case of a uniform distribution of caesium radionuclides in the body. The age-dependent calibration factors calculated for 17 radionuclides within the lungs are given for the DP-5 and the SRP-68–01 devices in Tables 7 and 8, respectively. The MCNP software was also used to calculate the device- and age-specific calibration factors for ^{131}I in thyroid (Table 9). These calibration factors were used to derive the ^{131}I activities in the thyroids from the results of the direct thyroid measurements. A detailed description of the calculations for the SRP-68–01 device can be found elsewhere (Khrutchinsky et al. 2012). Similar work was carried out for the DP-5 instrument.

Uncertainties of calibration factors given in Tables 6–9 are the same as those presented in Tables 4 and 5.

Comparison with other studies

Comparison with calibration factors derived from measurements of people— The calibration factor of the SRP-68–01 device for a mixture of ^{134}Cs and ^{137}Cs isotopes (activity ratio for^{134}Cs/^{137}Cs = 0.45) was determined by Kaidanovsky and Dolgirev (1997) from the results of measurements of exposure rate against the neck of six adult volunteers. The measurements were performed in St. Petersburg in the laboratory of radioisotope diagnostics. The calibration factor was found to be 1.56 ± 0.18 (kBq per counts s^{-1}). The value calculated in the present study for adult for ratio activities of ^{134}Cs to ^{137}Cs = 0.45 is equal to 1.63 ± 0.17 (kBq per counts s^{-1}) is consistent with the value of the calibration factor determined experimentally.

Comparison with other Monte Carlo calculations—Figure 4 compares the values of the calibration factors for the SRP-68–01 detector that have been calculated in the present study with those previously calculated (Ulanovsky et al. 2004). It should be noted that the values of the calibration factors used by Ulanovsky et al. (2004) were obtained for a detector positioned at mid-trunk. Consequently, there is a systematic difference between the calibration factors calculated in the two studies that is due to the different positions of the detectors.

Summary and Conclusions

A Monte Carlo method was used to calculate the response of thyroid detectors to external and internal contamination of the human body by radionuclides of Chernobyl origin. In Belarus, thyroid measurements were done in contaminated villages by un-collimated detectors and, as a rule, without measurements of background. Therefore, external and internal radioactive contamination of the measured individuals contributed to the response of the detector.

In the present study calibration factors were calculated for two detectors, the DP-5 device and the SRP-68–01 survey-meter, and for a broad list of radionuclides that caused external and internal contamination of the human body. To estimate the actual contribution of the radioactive contamination of the human body to the exposure rate measured near the thyroid gland, the radioactive contamination of the clothes and open surfaces of the human body as well as the activities incorporated in the body were assessed in a companion paper (Drozdovitch et al. 2019). The results presented in the two papers were combined to calculate the contributions of the external and internal contamination of the human body to the radiation signal, and, in turn, the ^{131}I activities in the thyroids of all individuals of an epidemiologic study of thyroid cancer and other thyroid diseases among 11,732 Belarusian-American cohort members who were exposed in childhood and adolescence.

Acknowledgements

This work was supported by the Intramural Research Program of the National Cancer Institute (NCI, USA), Division of Cancer Epidemiology and Genetics within the framework of the Belarus-U.S. Study of Thyroid Cancer and Other Diseases Following the Chernobyl Accident (Protocol #OH95-C-NO21); the ISTC Project #B-488p; the Intra-Agency Agreement between the National Institute of Allergy and Infectious Diseases (NIAID, USA) and the NCI, NIAID agreements #Y2-Al-5077 and #DCC-OD-12–900. The authors would like to thank Valery Kozhemyakin and Vladimir Guzov (SPE “Atomtex”, Minsk, Belarus), who contributed to the experimental estimation of the scaling coefficient of the devices.

Appendix:: Technique to accelerate Mont Carlo calculations for a radiation source uniformly distributed on a curved surface

Local weight procedure

To accelerate Monte Carlo calculations for a radiation source uniformly distributed on a body surface, a special procedure was developed that uses the local weight of the particle.

A uniformly contaminated curved surface area can be presented as a sum of elementary surface sources with activity proportional to their area. The weight w of each elementary surface source (weight of the particle) is determined by dividing its area by the total area of all elementary sources of a given area. In the proposed variant the value of w is not a constant for the particle in the given cell but is proportional to the area of the surface element $d\sigma(x,y,z)$ in photon position (x,y,z). If the surface is given parametrically $\boldsymbol{r}=\boldsymbol{r}$ (u, v) (u, v are the coordinates given on the surface), then the area element $d\sigma$ on it can be written as $d\sigma = w_L$*du*dv, where w_L can be used as the local weight of the particle at the point u, v on the surface.

Using equations of differential geometry (Korn and Korn 1968), the local weights for each type of body surface were found to be:

- $$\text{right circular cylinder (regions 3-6, u} = \varphi, \text{v} = \text{z}): \;\; w_L = r \qquad \text{(A1.1)}$$
- $$\text{ellipsoid (region 1, u} = \varphi, \text{v} = \theta): w_L = \sqrt{a^2 \cdot b^2 \cdot \cos^2\theta + c^2 \cdot \sin^2\theta \cdot \left(a^2 \cdot \sin^2\varphi + b^2 \cdot \cos^2\varphi\right)} \qquad \text{(A1.2)}$$
- $$\text{elliptic cylinder (regions 2,9–16,18,19, u} = \varphi, \text{v} = z): w_L = \sqrt{a^2 + \left(b^2 - a^2\right) \cdot \cos^2\theta} \qquad \text{(A1.3)}$$
- $$\text{parabolic cylinder (regions 7,8,17, u} = y, \text{v} = z): w_L = \cdot \sqrt{1 + 4 \cdot b_{sh}^2 \cdot \left(y - y_{0sh}\right)^2} \qquad \text{(A1.4)}$$

  where θ and φ are the polar and azimuth angles respectively. The azimuth angle was uniformly sampled in the interval (0,2π), while for the polar angle the quantity $\cos\theta$ was uniformly sampled in corresponding sectors.

In Eqs. (A1.2)–(A1.4) a, b, c are the semi-axes of the relevant ellipsoids or elliptic cylinders, r is the radius of right circular cylinder, in particular:

$$\begin{array}{l} \text{region 1 } a = a_h, b = b_h, c = c_{h2} \\ \text{regions 2,18,19 } a = a_h, b = b_h \\ \text{areas 3–6 } r = r_n \\ \text{areas 9–16 } a = a_t, b = b_t, \end{array} \qquad \text{(A1.5)}$$

where a_t and b_t are the body semi-axes, a_h and b_h are the head semi-axes, c_{h2} *is* the height of the elliptic head top, b_{sh}, y_{0sh} are parameters in Eq. A1.4 describing the parabolic shape of the trunk (Ulanovsky and Eckerman 1998), r_n is the radius of the neck. Values of parameters for the family of ORNL human phantoms are given in Table A1. The family of ORNL human phantoms are represented as erect with the position z-axis directed upward toward the head. The x-axis is directed to the phantom's left, and the y-axis is directed toward the posterior side of the phantom. The origin is taken at the center of the base of the trunk section of the phantom.

The result for a surface under consideration (tally in MCNP) was normalized to the sum of local weights for this surface. The validity of this procedure of using local weights was verified for regular surfaces such as sphere and circular cylinder, by comparison with the built-in MCNP values.

Table A1

Age-dependent parameters of whole body for the family of ORNL human phantoms (Cristy and Eckerman 1987).

Symbol[a]	**Value of parameters (cm) of whole body for phantom of age (y)**					
	Newborn	**1**	**5**	**10**	**15**	**20**
			Trunk parameters			
a_t	6.4	8.8	11.5	13.9	17.4	20.0
b_t	4.9	6.5	7.5	8.4	9.8	10.0
c_t	21.6	30.7	40.8	50.8	63.1	70.0
			Head parameters			
a_h	4.5	6.1	7.1	7.4	7.8	8.0
b_h	5.8	7.8	9.1	9.4	9.8	10.0
ch_1	7.0	9.5	10.7	11.7	12.4	13.1
ch_2	4.0	5.4	6.3	6.6	6.9	7.2
			Neck parameters			
r_n	2.8	3.6	3.8	4.4	5.2	5.4
ch_0	1.6	2.3	3.3	4.7	7.7	8.4
			Shoulders parameters			
dz_{sh}	1.0	1.5	2.0	2.8	4.5	5.0
b_{sh}	0.11	0.094	0.095	0.095	0.095	0.1
y_{0sh}	2.0	2.5	2.8	3.3	3.9	4.0
			Leg parameters			
c_{leg}	16.8	26.5	48.0	66.0	78.0	80.0
c'_{leg}	21.6	37.1	65.0	90.0	100	100

[a] a_t, b_t are trunk semi-major and semi-minor axes; c_t is height of trunk. Head parameters: ch_1 is height of lower part of head; ch_2 is height of upper part of head (head top); a_h, b_h are head top semi-major and semi-minor axes. Neck parameters: r_n is neck radius; ch_0 is height of neck of non-modified phantom. Shoulders parameters: dz_{sh} is modifying add to height of trunk in ORNL phantom; b_{sh} is coefficient at the parabolic term which describes the shape of the trunk in cm^{-1}; y_{0sh} is gap between the central axis of the trunk and the middle line of its parabolic shape. Leg parameters: c_{leg} is length of legs; c'_{leg} is length of cone that models legs.

Auxiliary means for improvement of calculation efficiency

It should be noted that the variance reduction technique cannot be applied to the spectrum tally F8 usually used for the SRP-68–01 device with a scintillation detector. For the DP-5 it was necessary to use flux tally (F1 in MCNP) instead of the spectrum (F8 in MCNP) and specify the relative cells importance in the sample problem to help particles move more easily to the important regions of the geometry. Such variance reduction technique for the DP-5 is matched with the FORTRAN sub-routine "source.f" which was developed for the implementation of the local weights approach.

To process the information from the MCNP results a special script, written in Perl language, was developed. This script arranges a cycle by desired energies from the list, inserting the required energy (and the corresponding number of histories) at each step of the cycle into the same input file. As soon as the MCNP code calculated the response function, the Perl script prepared a two-dimensional array (energy, response function) which was ready for use to calculate the calibration factor.

References

Briesmeister JF (1994) MCNP – A general Monte Carlo n-particle transport code. Version 4A. Report No LA-12625-M. Los Alamos National Laboratory; Radiation Shielding Information Center: Los Alamos, NM.

Cristy M (1980) Mathematical phantoms representing children of various ages for use in estimates of internal dose. Report No ORNL/NUREG/TM-367. Oak Ridge National Laboratory, Oak Ridge, TN.

Cristy M, Eckerman KF (1987) Specific absorbed fractions of energy at various ages from internal photon sources. Report No ORNL/TM-8381/V1. Oak Ridge National Laboratory, Oak Ridge, TN.

Drozdovitch V, Minenko V, Khrouch V, Leshcheva S, Gavrilin A, Khrutchinsky A, Kukhta T, Kutsen S, Luckyanov N, Shinkarev S, Tretyakevich S, Trofimik S, Voillequé P, Bouville A (2013) Thyroid dose estimates for a cohort of Belarusian children exposed to radiation from the Chernobyl accident. Radiat Res 179:597–609. [PubMed: 23560632]

Drozdovitch V, Minenko V, Golovanov I, Khrutchinsky A, Kukhta T, Kutsen S, Luckyanov N, Ostroumova E, Trofimik S, Voillequé P, Simon SL, Bouville A (2015) Thyroid dose estimates for a cohort of Belarusian children exposed to ^{131}I from the Chernobyl accident: assessment of uncertainties. Radiat. Res 184:203–218. [PubMed: 26207684]

Drozdovitch V, Khrouch V, Khrutchinsky A, Kutsen S, Minenko V, Shinkarev S, Konstantinov Yu, Gavrilin Yu, Luckyanov N, Voillequé P, Bouville A (2019) Influence of the external and internal radioactive contamination of the body and of the clothes on the results of the thyroidal 131I measurements conducted in Belarus after the Chernobyl accident. Part 1: Estimation of the external and internal radioactive contamination. Radiat Environ Biophys, this issue. DOI 10.1007/s00411-019-00784-3

Gavrilin YuI, Khrouch VT, Shinkarev SM, Krysenko NA, Skryabin AM, Bouville A, Anspaugh L, Straume T (1999) Chernobyl accident: reconstruction of thyroid dose for inhabitants of the Republic of Belarus. Health Phys 76:105–119. [PubMed: 9929121]

ICRP – International Commission on Radiological Protection (1983) Radionuclide Transformations - Energy and Intensity of Emissions. ICRP Publication 38. Ann. ICRP 11–13.

ICRP – International Commission on Radiological Protection (2008) Nuclear decay data for dosimetric calculations. ICRP Publication 107. Ann. ICRP 38 (3).

Kaidanovsky GN, Dolgirev EI (1997) Calibration of radiometers for mass control of incorporated ^{131}I, ^{134}Cs and ^{137}Cs nuclides with the help of volunteers. Radiat Prot Dosim 71:187–194.

Khrutchinsky A, Drozdovitch V, Kutsen S, Minenko V, Khrouch V, Luckyanov N, Voillequé P, Bouville A (2012) Mathematical modeling of a survey-meter used to measure radioactivity in human thyroids: Monte Carlo calculations of device response and uncertainties. Appl Radiat Isotopes 70:743–751.

Korn GA, Korn TM (1968) Mathematical handbook for scientists and engineers. McGraw-Hill, New York.

Likhtarev IA, Shandala NK, Goulko GM, Kairo IA, Chepurny NI (1993) Ukrainian thyroid doses after the Chernobyl accident. Health Phys 64:594–599. [PubMed: 8491614]

Likhtarev IA, Goulko GM, Sobolev BG, Kairo IA, Pröhl G, Roth P, Henrichs K (1995) Evaluation of the ^{131}I thyroid-monitoring measurements performed in Ukraine during May and June of 1986. Health Phys 69:6–15. [PubMed: 7790214]

Stezhko VA, Buglova EE, Danilova LI, Drozd VM, Krysenko NA, Lesnikova NR, Minenko VF, Ostapenko VA, Petrenko SV, Polyanskaya ON, Rzheutski VA, Tronko MD, Bobylyova OO, Bogdanova TI, Ephstein OV, Kairo IA, Kostin OV, Likhtarev IA, Markov VV, Oliynik VA, Shpak VM, Tereshchenko VP, Zamotayeva GA, Beebe GW, Bouville AC, Brill AB, Burch JD, Fink DJ, Greenebaum E, Howe GR, Luckyanov NK, Masnyk IJ, McConnell RJ, Robbins J, Thomas TL, Voillequé PG, Zablotska LB; Chornobyl Thyroid Diseases Study Group of Belarus, Ukraine, and the USA (2004) A cohort study of thyroid cancer and other thyroid diseases following the Chornobyl accident: objectives, design, and methods. Radiat Res 161:481–492. [PubMed: 15038762]

Ulanovsky A, Minenko V, Korneev S (1997) Influence of measurement geometry on the estimate of ^{131}I activity in the thyroid: Monte Carlo simulation of a detector and a phantom. Health Phys 72:34–41. [PubMed: 8972824]

Ulanovsky AV, Eckerman KF (1998) Modification of ORNL phantom series in simulation of the responses of thyroid detectors. Radiat Prot Dosim 79:429–432.

Ulanovsky A, Drozdovitch V, Bouville A (2004) Influence of radionuclides distributed in the whole body on the thyroid dose estimates obtained from direct thyroid measurements made in Belarus after the Chernobyl accident. Radiat Prot Dosim 112:405–418.

UNSCEAR – United Nations Scientific Committee on the Effects of Atomic Radiation Sources and Effects of Ionizing Radiation (2011) UNSCEAR 2008 Report. Annex D: Health effects due to radiation from the Chernobyl accident. Sales No. E.11.IX.3. New York: United Nations.

Zvonova IA, Balonov MI, Bratilova AA (1998) Thyroid dose reconstruction for population of Russia suffered after the Chernobyl accident. Radiat Prot Dosim 79:175–178.

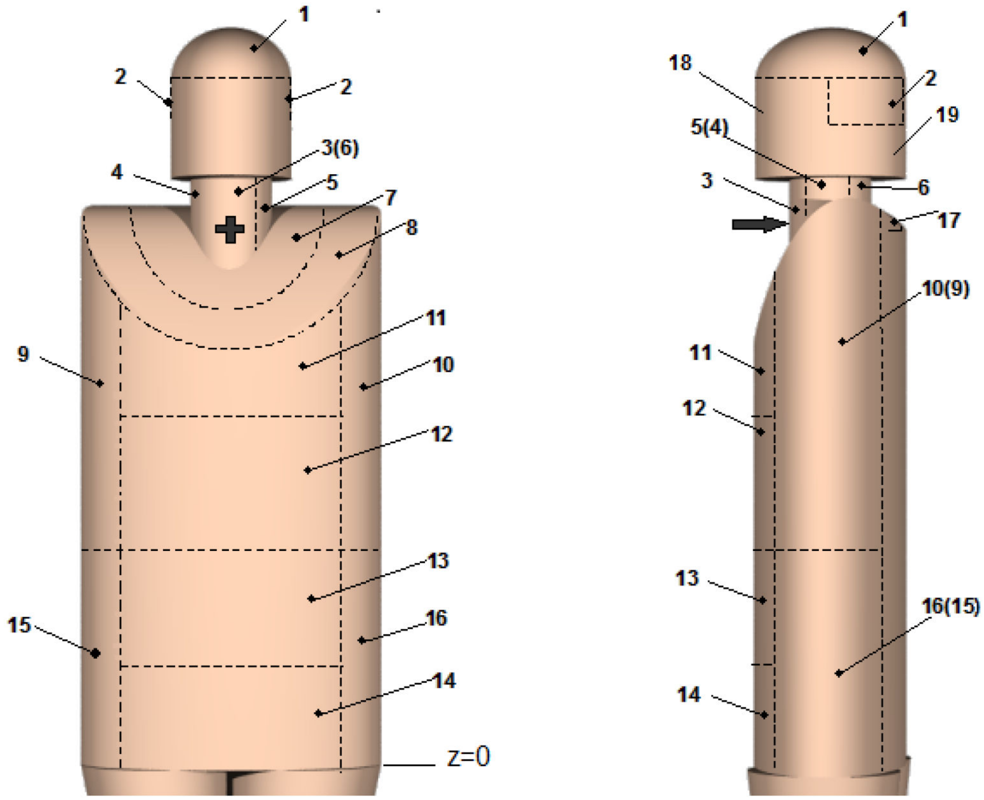

Fig. 1.

Division of phantom into regions (Ulanovsky et al. 2004): 1- top of the head; 2-sides of the head; 3-front side of neck; 4(5)-right (left) side of neck; 6-back of neck; 7-chest area close to the neck fragment of chest; 8-chest area more distant from the neck; 9(10)-upper right (left) arm; 11-front trunk (upper part); 12-front trunk (middle part 1); 13-front trunk (lower part 2); 14-front trunk (lower part); 15(16)-lower right (left) arm; 17-upper part of shoulder blades; 18-face; 19- occiput. Arrow indicates position of the thyroid detector during the measurement.

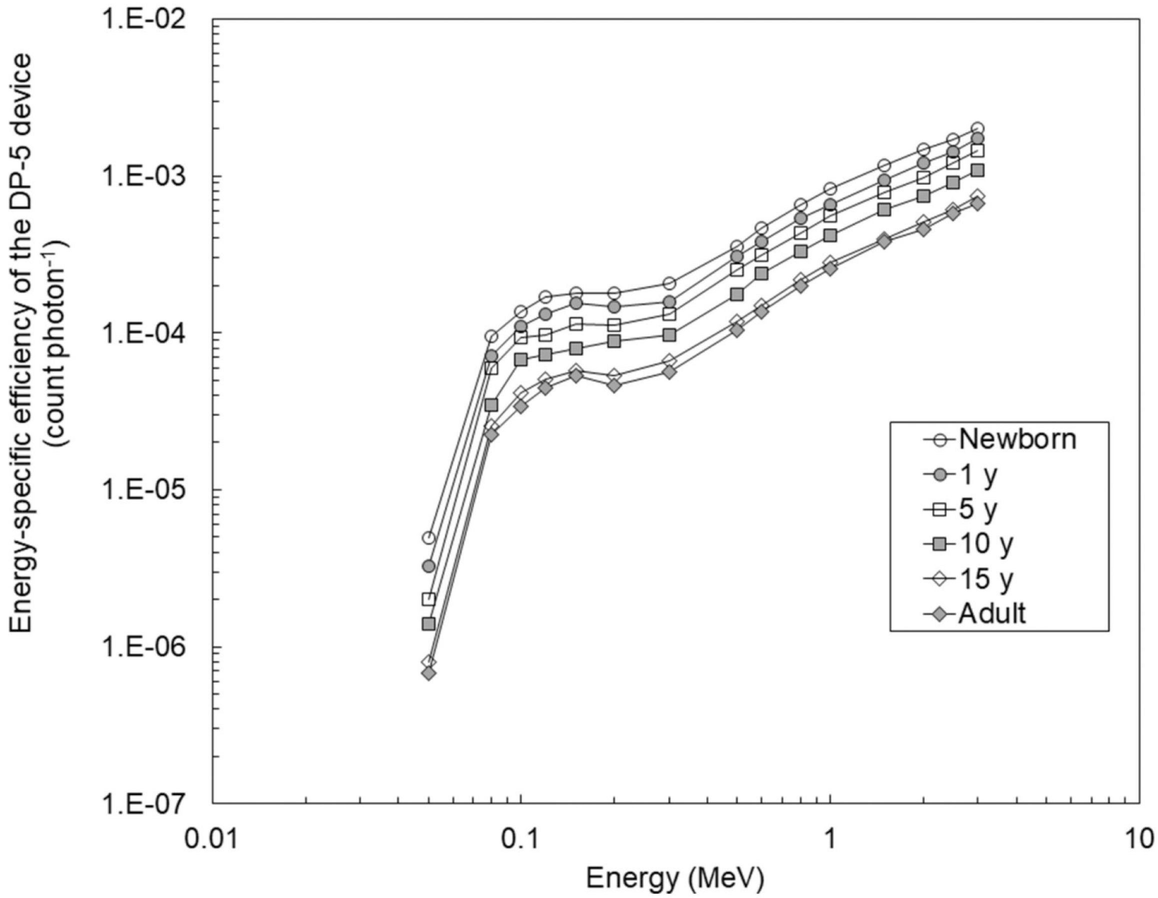

Fig. 2.
Energy-specific efficiency of the DP-5 device to radioactive contamination of the front surface of neck (region #3).

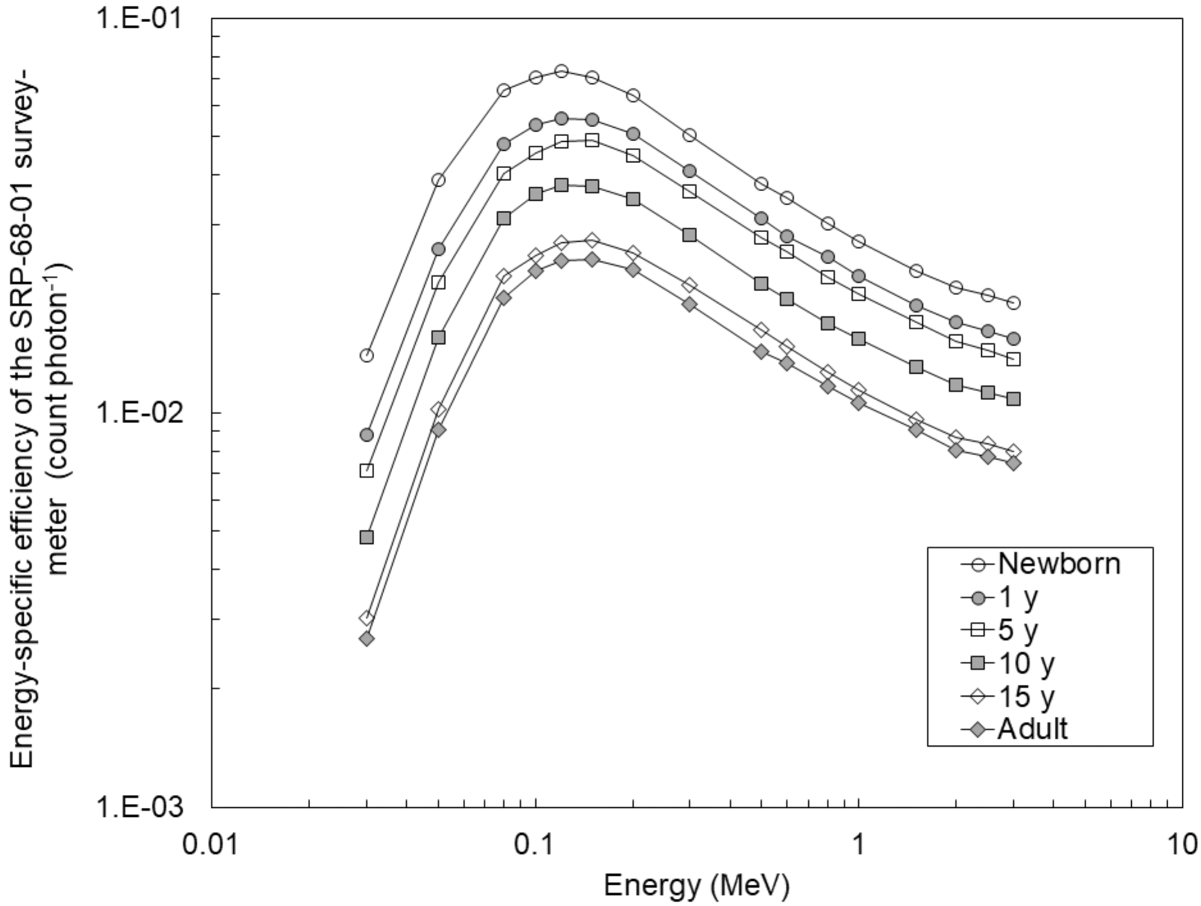

Fig.3.
Energy-specific efficiency of the SRP-68–01 survey-meter to radioactive contamination of the front surface of neck (region #3).

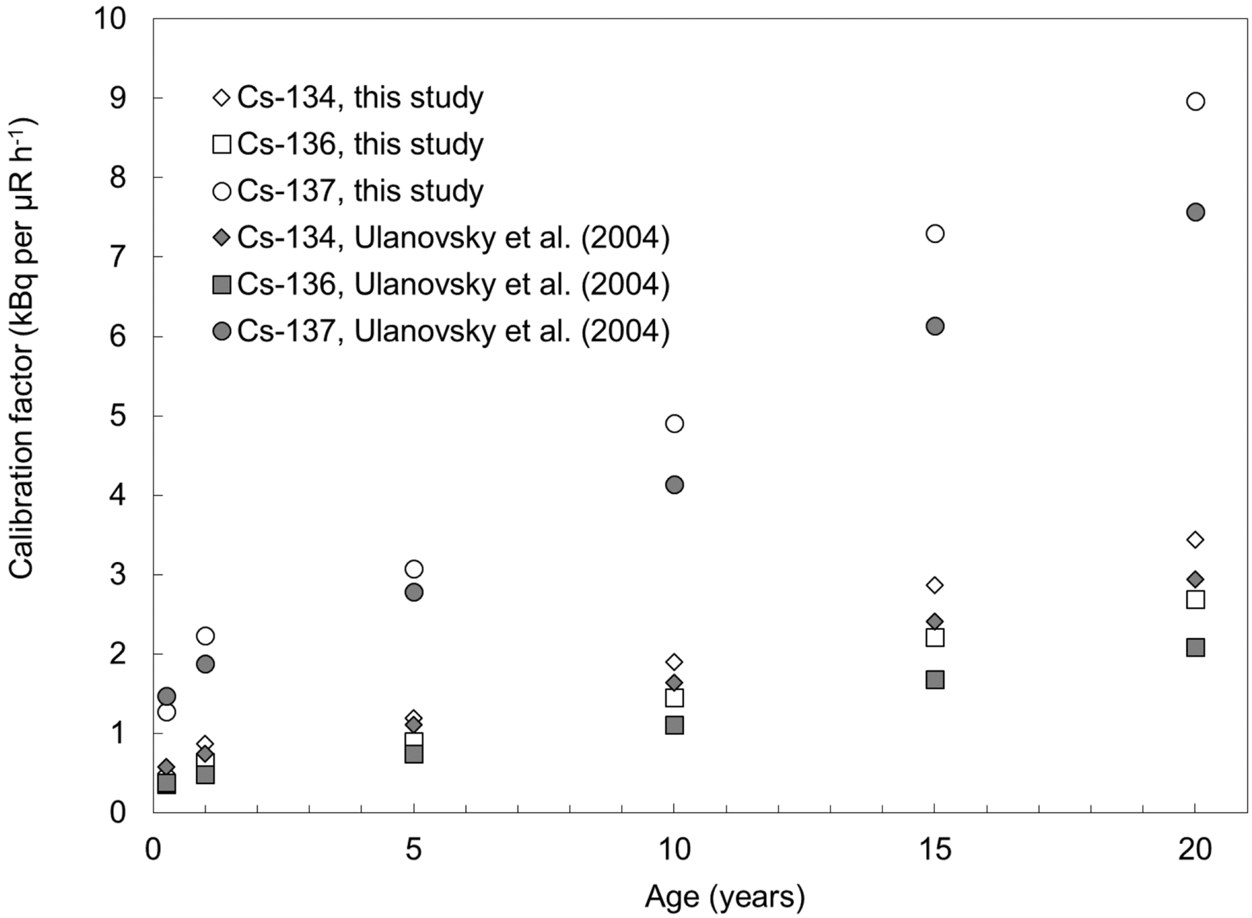

Fig. 4.
Comparison of calibration factors of the SRP-68–01 detector for caesium radionuclides uniformly distributed in the whole body calculated in by Ulanovsky et al. (2004) and in the present study.

Table 1

Area of the body surface regions for the family of ORNL human phantoms (Ulanovsky and Eckerman 1998). Numbers of body surfaces correspond to those shown in Fig. 1.

No	Name of body region	Area of body region (cm^2) of ORNL phantoms of age (y)					
		Newborn	1	5	10	15	Adult
1	Top of the head	142	261	351	381	415	440
2	Sides of the head	85	157	205	232	256	278
3	Front side of neck	12	22	30	48	83	96
4 (5)	Right (left) side of neck	5.1	9.1	14	23	41	47
6	Back of neck	3.6	6.3	9.2	15	26	30
7	Chest area close to the neck	30	57	93	137	218	274
8	Chest area more distant from the neck	38	76	134	197	317	403
9 (10)	Upper right (left) arm	376	735	1235	1839	2849	3559
11	Front trunk (upper part)	84	166	289	432	673	847
12	Front trunk (middle part 1)	48	94	161	240	368	468
13	Front trunk (lower part 2)	48	94	161	240	368	468
14	Front trunk (lower part)	48	94	161	240	368	468
15 (16)	Lower right (left) arm	57	108	170	242	357	421
17	Upper part of shoulder blades	23	46	75	100	148	175
18	Face	114	209	273	310	341	370
19	Occiput	29	52	68	78	85	93

Table 2

Age-dependent volumes of whole body, lung and thyroid gland for the family of ORNL human phantoms.

Age group (y)	Volume (cm^3)		
	Whole Body[a]	**Both Lungs[b]**	**Thyroid[a]**
Newborn	3,380	171	1.26
1	9,020	484	1.70
5	18,490	980	3.33
10	31,330	1,530	7.66
15	53,860	2,200	12.0
20 (adult)	70,330	3,380	20.0

[a](Ulanovsky and Eckerman 1998).

[b](Cristy and Eckerman 1987).

Author Manuscript

Author Manuscript

Author Manuscript

Table 3

DP-5 device-specific scale coefficients, *SC*, obtained experimentally for the different radiation sources.

Isotope	Activity (MBq)	Distance from the radiation source to the device surface (cm)	Measured dose rate (mR h^{-1})	*SC* (counts s^{-1} per μR h^{-1})
^{60}Co	280	100	7.5	0.0204
^{60}Co	280	83	10	0.0198
^{137}Cs	2,800	154	8.5	0.0197
Average				0.0200

Table 4

Calibration factors calculated for the DP-5device for radionuclides distributed on surfaces of human body for 5-y child. Numbers of body surfaces correspond to those shown in Fig. 1.

Radio-nuclide	Calibration factor for the DP-5 device (kBq per μR h^{-1}) for body surface #															
	1	2	3	4 (5)	6	7	8	9 (10)	11	12	13	14	15 (16)	17	18	19
^{95}Zr	2.8	2.7	0.05	0.25	0.66	0.12	0.33	2.7	1.0	6.0	19	57	30	1.1	0.84	1.3
^{95}Nb	2.5	2.6	0.05	0.24	0.63	0.11	0.31	2.5	0.97	5.6	18	53	28	1.1	0.80	1.2
^{99}Mo	9.2	6.7	0.11	0.57	1.5	0.27	0.76	7.6	2.4	18	68	210	115	2.6	2.0	2.9
^{103}Ru	6.5	4.5	0.08	0.38	1.2	0.21	0.59	4.9	1.8	11	42	115	64	2.0	1.4	2.1
^{106}Ru	14	10	0.19	0.88	2.7	0.45	1.3	11	3.8	23	81	220	115	4.4	3.2	4.7
^{132}Te	19	9.4	0.20	0.83	2.5	0.46	1.2	12	4.2	28	120	480	185	4.0	3.4	4.0
^{131}J	7.8	6.0	0.11	0.53	1.5	0.28	0.74	6.9	2.5	14	55	180	95	2.5	1.8	2.8
^{132}J	0.99	0.86	0.02	0.08	0.22	0.04	0.10	0.88	0.31	1.9	5.9	17	8.8	0.36	0.27	0.41
^{133}J	4.7	3.5	0.06	0.30	0.92	0.15	0.43	3.8	1.3	8.0	28	78	41	1.5	1.1	1.6
^{134}Cs	1.4	1.3	0.02	0.12	0.33	0.06	0.16	1.3	0.48	2.9	9.6	27	14	0.55	0.41	0.61
^{136}Cs	0.97	0.89	0.02	0.1	0.23	0.04	0.11	0.87	0.31	1.8	5.8	17	8.6	0.37	0.28	0.43
^{137}Cs	5.2	3.7	0.07	0.33	0.94	0.16	0.43	3.9	1.4	8.5	28	82	41	1.6	1.2	1.7
^{140}Ba	18	12	0.21	0.99	3.0	0.52	1.4	13	4.5	29	109	310	165	5.0	3.6	5.4
^{140}La	0.95	0.8	0.02	0.08	0.22	0.04	0.10	0.87	0.27	1.6	4.4	11	6.5	0.34	0.25	0.40
^{141}Ce	46	24	0.37	1.9	5.3	0.89	2.6	30	7.9	74	365	1215	695	8.7	6.7	10
^{144}Ce	54	37	0.70	3.4	9.6	1.6	4.4	42	13	82	255	660	390	15	12	17
^{239}Np	40	20	0.35	1.6	4.9	0.88	2.3	26	8.3	59	260	1050	440	8.0	6.4	8.3

Table 5

Calibration factors calculated for the SRP-68–01 survey-meter for radionuclides distributed on surface of human body for 5-y child. Numbers of body surfaces correspond to those shown in Fig. 1.

Radio-nuclide	Calibration factor for the SRP-68–01 survey-meter (kBq per μR h^{-1}) for body surface #															
	1	2	3	4 (5)	6	7	8	9 (10)	11	12	13	14	15 (16)	17	18	19
^{95}Zr	6.9	3.9	0.16	0.50	1.1	0.38	0.65	3.2	1.5	6.2	17	46	32	1.5	1.5	2.3
^{95}Nb	6.9	3.9	0.16	0.50	1.1	0.38	0.66	3.2	1.5	6.1	16	45	31	1.5	1.5	2.3
^{99}Mo	7.2	3.3	0.07	0.30	0.73	0.19	0.32	2.7	0.91	5.6	19	48	50	1.0	0.85	1.4
^{103}Ru	6.9	3.8	0.14	0.49	0.98	0.32	0.56	3.0	1.3	5.9	18	44	35	1.4	1.3	2.0
^{106}Ru	20	11	0.41	1.4	2.8	0.97	1.7	8.7	4.0	17	50	125	96	4.1	3.8	6.0
^{132}Te	7.5	3.6	0.08	0.34	0.82	0.22	0.38	2.7	1.0	5.9	21	52	57	1.1	0.99	1.6
^{131}J	6.8	3.5	0.11	0.42	0.87	0.27	0.46	2.7	1.2	5.6	18	43	36	1.2	1.1	1.8
^{132}J	2.3	1.3	0.05	0.17	0.35	0.12	0.21	1.1	0.49	2.0	5.6	15	11	0.5	0.48	0.74
^{133}J	6.5	3.6	0.13	0.47	0.93	0.32	0.54	2.9	1.3	5.6	17	41	32	1.4	1.3	2.0
^{134}Cs	3.1	1.7	0.07	0.23	0.46	0.16	0.28	1.4	0.65	2.7	7.4	20	15	0.66	0.62	0.97
^{136}Cs	2.4	1.3	0.04	0.16	0.34	0.11	0.19	1.1	0.46	2.1	5.9	15	11	0.48	0.44	0.69
^{137}Cs	8.0	4.5	0.17	0.58	1.2	0.42	0.72	3.6	1.7	7.1	19	53	40	1.7	1.6	2.5
^{140}Ba	16	8.6	0.25	0.98	2.1	0.65	1.1	6.7	2.8	14	41	105	87	3.0	2.7	4.3
^{140}La	3.4	1.9	0.08	0.26	0.53	0.18	0.31	1.6	0.72	3.0	8.2	19	14	0.75	0.7	1.1
^{141}Ce	17	7.6	0.14	0.62	1.6	0.41	0.69	6.2	2.0	13	45	120	135	2.3	1.9	3.1
^{144}Ce	78	32	0.52	2.4	6.3	1.6	2.8	27	8.4	58	210	500	650	9.1	7.8	13
^{239}Np	16	7.3	0.16	0.65	1.6	0.41	0.70	5.6	2.0	12	43	105	120	2.3	1.9	3.1

Table 6

Age-dependent calibration factors for caesium radionuclides distributed in the human body.

Age, year	Calibration factor (kBq per μR h^{-1}) for the detector located in standard position[a]					
	DP-5			SRP-68–01		
	^{134}Cs	^{136}Cs	^{137}Cs	^{134}Cs	^{136}Cs	^{137}Cs
Newborn	0.27	0.18	0.79	0.49	0.36	1.27
1	0.52	0.35	1.47	0.87	0.64	2.23
5	0.90	0.61	2.53	1.19	0.90	3.08
10	1.36	0.92	3.79	1.90	1.45	4.91
15	2.22	1.51	6.36	2.87	2.21	7.30
20 (adults)	2.75	1.91	7.83	3.44	2.69	8.97

[a]Detector is located at lower point of neck

Table 7

Calibration factors calculated for the DP-5 device for radionuclides within the lungs.

Radionuclide	Calibration factor for the DP-5 (kBq per μR h^{-1}) for age group (y)					
	Newborn	1	5	10	15	Adult
^{95}Zr	0.32	0.57	0.89	1.2	2.2	2.5
^{95}Nb	0.31	0.54	0.85	1.1	2.1	2.4
^{99}Mo	0.73	1.3	1.9	2.9	5.3	6.1
^{103}Ru	0.56	1.0	1.3	2.1	3.8	4.1
^{106}Ru	1.2	2.2	3.1	4.7	8.3	9.1
^{132}Te	1.1	1.9	2.8	4.1	7.2	8.7
^{131}J	0.71	1.2	1.7	2.7	4.8	5.3
^{132}J	0.10	0.18	0.28	0.39	0.70	0.78
^{133}J	0.43	0.75	1.1	1.6	2.9	3.1
^{134}Cs	0.16	0.27	0.43	0.58	1.1	1.2
^{136}Cs	0.11	0.19	0.28	0.41	0.72	0.81
^{137}Cs	0.44	0.77	1.2	1.6	2.9	3.3
^{140}Ba	1.4	2.5	3.4	5.3	9.5	10
^{140}La	0.10	0.17	0.26	0.36	0.65	0.72
^{141}Ce	2.5	4.1	6.1	10	19	21
^{144}Ce	11	20	30	48	90	110
^{239}Np	2.1	3.8	5.5	8.4	16	18

Table 8

Calibration factors calculated for the SRP-68–01 device for radionuclides within the lungs.

Radionuclide	Calibration factor for the SRP-68–01 (kBq per μR h^{-1}) for age group (y)					
	Newborn	1	5	10	15	Adult
^{95}Zr	0.80	1.1	1.5	1.9	2.7	3.0
^{95}Nb	0.80	1.1	1.5	1.8	2.7	3.0
^{99}Mo	0.43	0.61	0.9	1.3	2.0	2.2
^{103}Ru	0.70	0.95	1.3	1.7	2.4	2.6
^{106}Ru	2.1	2.8	3.8	5.0	7.2	7.8
^{132}Te	0.5	0.72	1.0	1.4	2.1	2.4
^{131}I	0.59	0.82	1.1	1.5	2.2	2.4
^{132}I	0.26	0.36	0.48	0.62	0.89	0.98
^{133}I	0.68	0.93	1.2	1.6	2.4	2.6
^{134}Cs	0.34	0.47	0.63	0.81	1.2	1.3
^{136}Cs	0.23	0.33	0.44	0.59	0.86	0.96
^{137}Cs	0.88	1.2	1.6	2.1	3.0	3.3
^{140}Ba	1.4	2.0	2.7	3.6	5.4	5.9
^{140}La	0.38	0.53	0.7	0.92	1.3	1.4
^{141}Ce	0.92	1.3	2.0	2.8	4.4	5.0
^{144}Ce	3.7	5.5	8.3	12	19	22
^{239}Np	0.95	1.4	2.0	2.7	4.3	4.8

Table 9

Calibration factors for ^{131}I for the thyroid detectors that were used in Belarus to derive the ^{131}I activity in the thyroid from the direct thyroid measurements.

Age group (y)	Calibration factor for the device (kBq per μR h^{-1})	
	DP-5	SPR-68–01
Newborn	0.190	0.98
1	0.185	0.100
5	0.200	0.110
10	0.285	0.126
15	0.390	0.147
20 (adult)	0.450	0.167